Harvesting Information Extraction using Sentinel-2 and CubeSat temporal data for Medicinal Psyllium Husk Crop

Anam Sabir*, and Anil Kumar
Indian Institute of Remote Sensing, Dehradun, India
*Email: anamsabir1331@gmail.com

(Received: Dec 05, 2021; in final form Feb 28, 2022)

Abstract: Harvesting information is required for a number of applications for example to maximize crop yield, minimize crop losses, quality deterioration assessment, crop health assessment and phenological studies. This study was carried out for the mapping of Psyllium Husk crop fields harvested on different dates in Jalore district of Rajasthan, India. Jalore district region is famous for various other medicinal/spice crop fields in addition to Psyllium Husk such as cumin, fenugreek, castor, etc. Therefore, in order to highlight the target crop, a temporal dataset was prepared using MSAVI2 (Modified Soil Vegetation Index) to incorporate the whole phenology of the crop that serves as a unique signature for separating it from non-target crops. Two variants of MSAVI2 index were tested for extracting the harvest information i.e., Conventional MSAVI2 and CBSI-MSAVI2 (Class Based Sensor Independent). To improve the extraction of harvesting information at 3 to 4 days interval, optical data of CubeSat (3m) was incorporated along with that of Sentinel (10m) temporal data for refining the temporal resolution. The harvested Psyllium Husk crop fields were mapped using Fuzzy MPCM (Modified Possibilistic c-means) classifier using two approaches under varied sample sizes for training dataset. The best combination of index, MPCM approach and number of training samples were taken into consideration for the extraction of field harvesting information. Accuracy assessment of results obtained was done on the basis of MMD (Mean Membership Difference) and variance within the field. CBSI results showed more homogeneity within the crop with minimum variance, while both the combinations of index and classification approach i.e. Mean MPCM with MSAVI2 and Individual-sample-as-mean MPCM as CBSI-MSAVI2 gave satisfactory results.

Keywords: MSAVI2, CBSI-MSAVI2, Fuzzy MPCM (Modified Possibilistic c-Means), Psyllium Husk crop

1. Introduction

Satellite images prove useful for various applications in different domains, one of the major one being agriculture. There are a number of practices and studies such as crop condition monitoring (Villa et al., 2015), yield estimation etc. which focus on a specific crop and hence require specific crop mapping. In order to highlight a particular class among different fields present in the area of interest, multi-temporal information is required. There have been studies which incorporate data acquired on a number of dates which forms a basis for the detection of a particular crop with the help of phenological information extracted (Ennouri et al., 2019; Sun et al., 2019; Zhou et al., 2018). Medicinal crops are of great importance and have a significant contribution in the economy due to export business. Whereas since there is less awareness about them, they are often left unidentified (Biswas et al., 2017) which leads to wastage of a valuable resource. Use of satellite data for medicinal crop mapping serves as an efficient way as it has no constraint of area and time series data can be utilized for phenological (Murugan et al., 2016) and crop health monitoring studies (Villa et al., 2015). Very few studies have explored the mapping of medicinal crops using remote sensing (Biswas et al., 2017; Sinha & Singh, 2011).

Psyllium Husk is a medicinal herb (scientific name: Plantago Ovata). It is grown in Mediterranean region and West Asia. It is short stemmed and attains a height around 30-40cm and requires cool and dry weather ensuring no rain for crop maturity. It takes around 110-120 days to mature when the leaves turn yellowish and spikes turn brownish in colour with dark brown seeds exposed (Masood & Miraftab, 2010).

Different vegetation indices which are used for crop mapping include NDVI (Normalized Difference Vegetation Index), EVI (Enhanced Vegetation Index), SAVI (Soil Adjusted Vegetation Index) etc. (Almutairi et al., 2013). The choice of index depends on the crop and area under study. NDVI is appropriate for crops or vegetated areas, which are uniform and dense in nature. Thus, it has been tested for crops such as wheat (Sun et al., 2019) and Paddy (Salmon et al., 2015) etc. It is the most commonly used vegetation index for vegetation studies. Although NDVI has some disadvantages such as sensitivity to background reflectance and saturation at higher leaf area. To overcome this issue, EVI is used which incorporates an extra blue wavelength band. If the crop structure is discontinuous and the top view of field has more exposure of soil, SAVI (Huete, 1996) and its other forms such as MSAVI and MSAVI2 (Qi et al., 1994) are preferred as they reduce the effect of soil brightness from the response received by the sensor. Whereas while incorporating more wavelength bands, EVI is used. It has improved sensitivity to high biomass regions. This in turn increases the amount of information content being deduced from the remote sensing data.

On the other side, for extraction of classes, a range of classification algorithms is available for application on satellite imagery. There are two types of classifications on the basis of output i.e. hard and soft. Hard classification refers to the kind in which output is either zero or one for all the pixels present in the image. Either they get fully classified in a particular class or not at all. There is no partial membership or belonging in any class. This increases the amount of error for real life applications since most of the pixels are not pure in nature i.e. they are

comprised of different classes hence affecting the behaviour they exhibit. To handle this, the second kind of classification is used i.e. soft classification. It generates fractional images as output, which correspond to the degree of belongingness of a pixel in more than one number of classes, thus fitting the real life scenario more appropriately.

There is a range of Fuzzy classifiers to choose from according to the application, the basic one being Fuzzy c-means classifier (FCM) which was introduced by Dunn (1973) and has further been developed by Bezdek et al., 1984. Here sum of all membership values for a pixel (that for each class under consideration) is one. Hence, it is unable to extract a single class from an image. To overcome this disadvantage (hyperline constraint), Possibilistic c-means classifier (PCM) (R Krishnapuram & Keller, 1993) was developed in which this constraint was removed and hence it was able to extract a single class too. Whereas it shows an error of coincident clusters in the output which was further eliminated using Modified Possibilistic c- means classifier (MPCM) (Raghu Krishnapuram & Keller, 1996).

2. Vegetation Index and Classification Algorithm

2.1 MSAVI2

The vegetation index used for the study is MSAVI2 (Modified Soil Vegetation Index) which reduces the impact of soil brightness on the pixel value. This is required because the crop is not dense and continuous in structure thus increasing the soil exposure in the ground coverage. This in turn has a considerable impact on the reflectance from the ground. Therefore, to suppress soil exposure' impact, MSAVI2 is utilized. The formula for MSAVI2 is as given in equation (1).

$$MSAVI2_{Conv} = \frac{(2*NIR+1-\sqrt{(2*NIR+1)^2-8*(NIR-Red)})}{2} \quad (1)$$

2.1.1 CBSI MSAVI2

The CBSI approach is used for highlighting the target feature irrespective of the wavelength bands since it is not necessary that the bands in conventional formulae of indices are the most appropriate bands. Hence bands may be selected from the range available according to the application (Verrelst et al., 2016; Zhang et al., 2017). It picks up the bands which have minimum and maximum values for the target feature and utilizes it for calculating the index using its original formula, but with the bands extracted by it. This maximizes the values of index for the target feature hence resulting in better differentiation from background or other similar features. The formula for CBSI-MSAVI2 is as given in equation (2)

$$MSAVI2_{CBSI} = \frac{(2*Max+1-\sqrt{(2*Max+1)^2-8*(Max-Min)})}{2} \quad (2)$$

2.2 Classification Algorithm

The classification algorithm applied in this study is Modified Possibilistic c-means (MPCM) (Raghu Krishnapuram & Keller, 1996). MPCM is a fuzzy classification algorithm, which gives fractional images as outputs i.e. images with pixel values as membership values of that respective pixel for the target class. Hence the number of outputs depends on the number of classes, one fractional image for each class. This algorithm has the ability to work on mixed pixels (those that are composed of more than one class and exhibit partial behavior accordingly), to extract one single class from the image (independent on the number of classes) and to handle noise and outliers efficiently. The objective function of MPCM is given in equation (3).

$$J_{MPCM}(U,V) = \sum_{j=1}^{c}\sum_{i=1}^{N}\mu_{ij}^{m}d_{ij}^{2} + \eta_j\sum_{i=1}^{N}(\mu_{ij}log\mu_{ij} - \mu_{ij}) \quad (3)$$

Here, U is the matrix containing membership values for each pixel corresponding to each class while V is the matrix containing class centers. Rest of the parameters in the above equation are explained as follows separately along with respective formulae.

μ_{ij} is the typicality value of pixel i in class j and is given by equation (4).

$$\mu_{ij} = exp(-d_{ij}^2/\eta_j), \text{ for all i,j} \quad (4)$$

d_{ij}^2 the square of the distance between the measured value of a pixel and that of cluster centre. It is given as equation (5).

$$d_{ij}^2 = \|x_i - v_j\|^T A^{-1}(x_i - v_j \quad (5)$$

In the above equation, x_i refers to the measured value whereas v_j is the cluster centre which is given as equations (6) and (7) respectively.

$$\mu_{ij} = exp(-d_{ij}^2/\eta_j), \text{ for all i,j} \quad (6)$$

$$v_j = \frac{\sum_{i=1}^{N}\mu_{ij}x_i}{\sum_{i=1}^{N}\mu_{ij}} \quad (7)$$

3. Study Area and Data Used

The area under study comprises parts of Jalore and Badmer districts of Rajasthan, India. This area is known for crop fields and has a variety of medicinal crops as well. A field visit was carried to this area for collection of ground truth data. Geo-locations of different points on various crops were recorded. The crops present in the study area include Psyllium Husk, Cumin, Fenugreek, Castor, Wheat, Mustard, etc. One of the advantages of considering this particular area for satellite image analysis is that it is free from haze and cloud coverage majority of the time. This improves the contrast in the image making visual interpretation as well as digital image analysis easier and more efficient. Figure 1 shows the map and location of the study area.

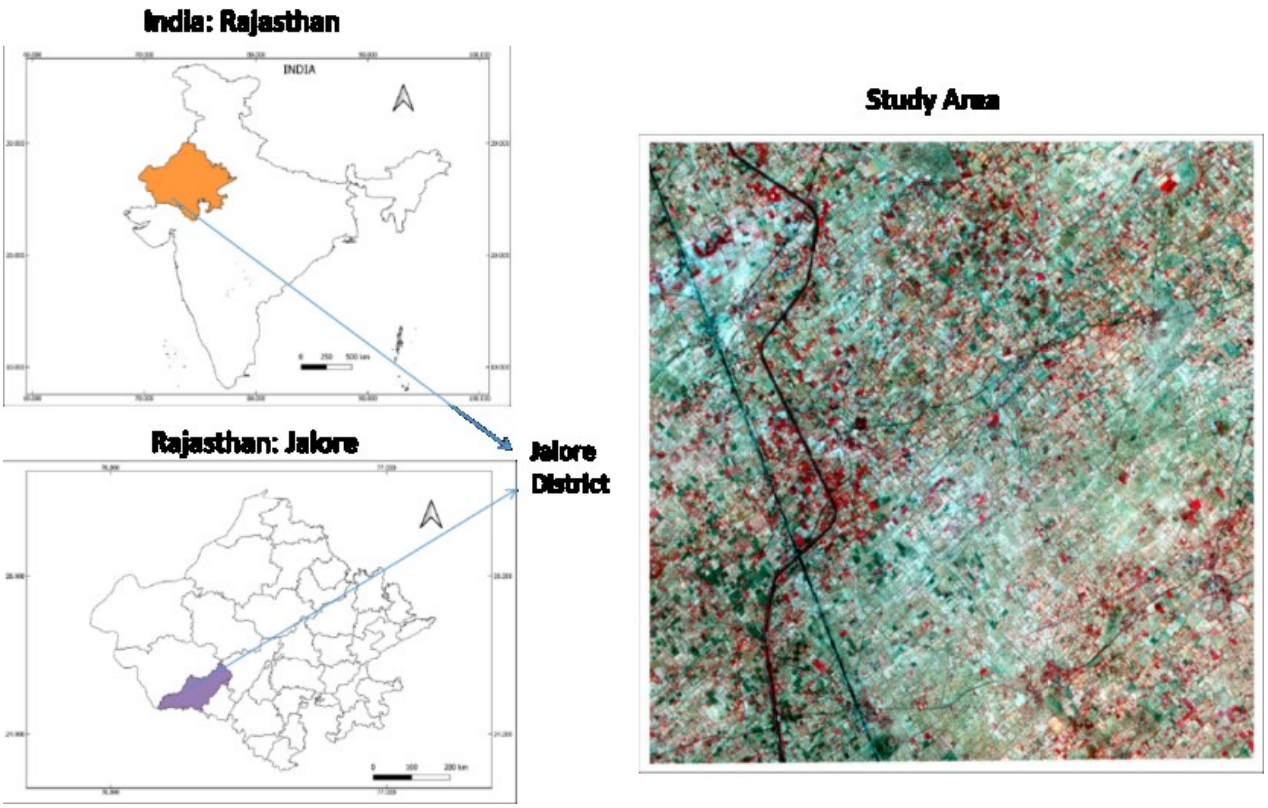

Figure 1. Study Area

For monitoring crop stages, temporal data was required which may be in interval of around one week. But if the study focuses on one particular crop harvesting stage, the temporal resolution required should be finer. The harvest dates are very close to each other due to the weather in Rajasthan which gets very hot in the month of March resulting in rapid ripening of target crop. Thus, the difference in dates of early and late harvest crops was very less which calls for a dataset that incorporates fine temporal resolution data for the mapping of harvested fields. For this, Sentinel-2 data with temporal resolution 5 days and CubeSat data with temporal resolution 1 day was utilized. The satellite data specifications are as listed in Table 1.

Table 1. Data Specifications

Sentinel-2 (A & B)	Spatial Resolution	10m
	Temporal Resolution	5 Days
	Data Source	Copernicus Open Access Hub
	Spectral Bands	13 (10 bands used with spatial resolution 10m and 20 m) Band 2-Blue (490 nm) [10m] Band 3-Green (560 nm) [10m] Band 4-Red (665 nm) [10m] Band 5-Red edge (705 nm) [20m] Band 6-Red edge (740 nm) [20m] Band 7-Red edge (783 nm) [20m] Band 8-NIR (842 nm) [10m] Band 8A-Red Edge (865 nm) [20m] Band 11-SWIR (1,610 nm) [20m] Band 12-SWIR (2,190 nm) [20m]
CubeSat	Spatial Resolution	3m
	Temporal Resolution	1 Day
	Data Source	PlanetScope
	Spectral Bands	4 (all 4 bands used) Band 1- Blue (455 - 515 nm) [3m] Band 2- Green (500 - 590 nm) [3m] Band 3- Red (590 - 670 nm) [3m] Band 4- Near Infrared (780 - 860 nm) [3m]

Psyllium husk is a Rabi crop and grown in dry regions. It is sown in November or December and harvested in the month of March. The crop cycle is of around 110-120 days. The specific crop stages according to the corresponding dates are listed below in Table 2.

Table 2. Psyllium Husk Crop Stages

Month	Crop Stage
November	Sowing
December	Seeding
January	Budding
February	Flowering
March	Harvesting

The various dates taken for the study are listed in Table 3 along with the corresponding crop stages.

Table 3. Temporal Dataset Details

Dates (2021)	Crop Stage/Status
14th February	Fully vegetated
1st March	Ripening initiated
16th March	Maturing
21st March	Harvest 1
24th March	Harvest 2
27th March	Harvest 3

4. Methodology

The optical data downloaded from Copernicus and PlanetScope was pre-processed for compatibility. The optical data from Sentinel-2 was available in 13 bands, out of which bands with 60m spatial resolutions were left out and bands with 10m and 20m spatial resolution were considered for the study. The selected Sentinel-2 bands were resampled to 3m pixel size to match with CubeSats' spatial resolution. In case of CubeSat data, since the data for an area under study was not covered in one scene, the individual images were mosaiced. The proposed methodology is shown in Figure 2.

Specific crop mapping was conducted for two forms of MSAVI2 index, first of them being the conventional (making use of Red and NIR bands) while the other was based on CBSI (Class Based Sensor Independent) approach. Hence two sets of MSAVI2 were generated for each of the image corresponding to dates under consideration.

Apart from this, two variants of MPCM algorithms were tested, mean based and individual-sample-as-mean based, to compensate for the heterogeneity within target crop. A range of training samples were made use of and tested for the mapping of Psyllium Husk crop. The training sample size was made to vary between 5 and 50.

Out of various dates considered throughout the season of the target crop, optimum dates were selected with the help of separability analysis. This was done in order to reduce the database size by decreasing redundancy and also maximizing spectral gap between target and non-target crops. Thus, the dates, which gave maximum value for minimum spectral difference between Psyllium Husk and the crop most similar to it, which came out to be Fenugreek, were taken forward for further analysis. The optimum dates thus selected are essential for mapping of target crop and are sufficient to distinguish it from the non-target crops present in the scene. These optimum dates came out to be 31st Dec 2020, 10th Jan 2021, 4th Feb 2021, 1st Mar 2021 and 26th Mar 2021 for mapping target crop Psyllium Husk. The MSAVI2 database of optimum dates were then stacked together to further run a Fuzzy MPCM (Modified Possibilistic c-Means) classification algorithm with the test cases as shown in Table 4.

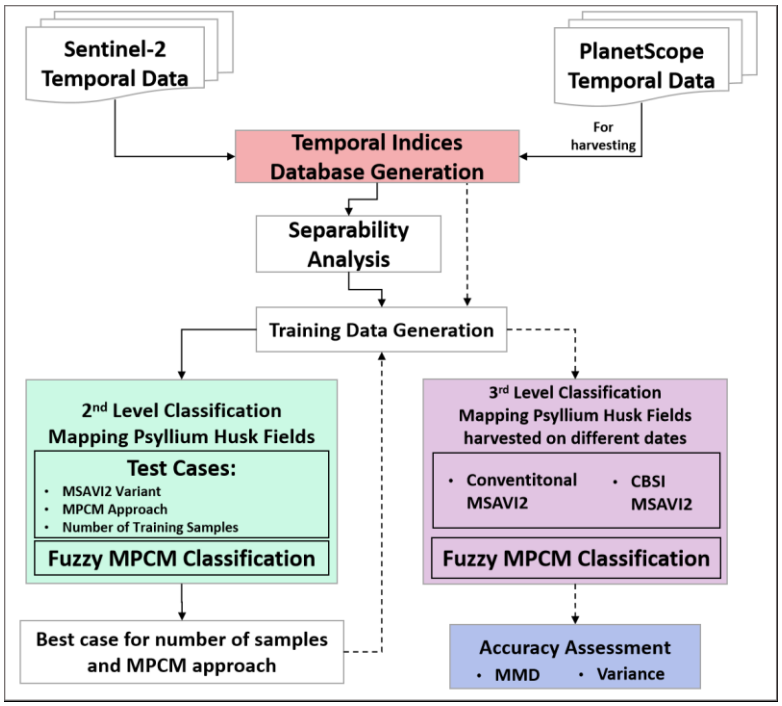

Figure 1. Proposed Methodology

Table 4. Test Cases for Psyllium Husk Crop Mapping

Algorithm	Approach	Index	Number of samples
MPCM	Mean	MSAVI2 MSAVI2- RedEdge CBSI MSAVI2	5, 10, 15. 20, 25, 50
MPCM	Individual Sample as Mean	MSAVI2 MSAVI2- RedEdge CBSI MSAVI2	5, 10, 15. 20, 25, 50

The most appropriate combination of approach and number of samples were selected i.e. those, which efficiently mapped all the Psyllium Husk fields with distinct boundaries and homogeneous enclosed area. These combinations of approach and number of samples for conventional MSAVI2 index as well as CBSI-MSAVI2 were carried on for the harvest study as described in Table 5. The RedEdge MSAVI2 index was dropped due to the unavailability of RedEdge band in CubeSat data.

The dates under consideration for harvest were selected and added to the dataset one by one. Training samples were marked according to the ground truth for various dates on which harvesting was observed using CubeSat data. The algorithm was run to extract all the Psyllium Husk fields, which were harvested on those dates using the phenological curves thus obtained. The harvested fields from 21st March 2021 to 27th March 2021 were mapped on an interval of 3 days. It was observed that harvesting in all the fields was done within in a span of 10 days. The harvesting dates observed were 21st March, 24th March and 27th March. Three databases corresponding to the three harvest dates were prepared with MSAVI2 and CBSI-MSAVI2 files of dates starting from the peak of phenological curve of Psyllium Husk i.e. the date with maximum vegetation (hence maximum MSAVI2 values) which is 14th Feb 2021 to the specific harvest date. The dates taken for the preparation of these datasets are listed in Table 6

The bands used for preparation of CBSI-MSAVI2 files have been listed in Table 7 for each date considered in harvesting information extraction. It includes the maximum and minimum valued band along with thus computed MSAVI2 value.

The curves obtained for the three databases prepared for each harvest date can be seen in Figure 3 where each curve corresponds to the harvest on 21st, 24th and 27th March 2021. As CBSI approach takes care of each date and gives maximum index (CBSI-MSAVI2) value for the target crop, it can be seen that the curve has less slope and is elevated. This further facilitates the mapping of harvested Psyllium Husk crop fields.

Table 5. Input and Approach selected for Harvest Information Extraction within Psyllium Husk Crop Fields

Algorithm	Approach	Index	Number of samples
MPCM	Mean	MSAVI2	15
MPCM	Individual Sample as Mean	CBSI-MSAVI2	10

Table 6. Temporal data used for Harvested Fields Extraction

Harvest Date	Temporal Data
21st Mar 2021	14th Feb 2021, 1st Mar 2021, 16th Mar 2021, 21st Mar 2021
24th Mar 2021	14th Feb 2021, 1st Mar 2021, 16th Mar 2021, 21st Mar 2021, 24th Mar 2021
27th Mar 2021	14th Feb 2021, 1st Mar 2021, 16th Mar 2021, 21st Mar 2021, 24th Mar 2021, 27th Mar 2021

Table 7. Temporal data used for Harvested Fields Extraction

Date	Satellite Data Used	Maximum Valued Band	Minimum Valued Band	MSAVI2 Value
31st Dec 2020	Sentinel	SWIR (Band 11)	Blue (Band 2)	0.6539
10th Jan 2021	Sentinel	SWIR (Band 11)	Blue (Band 2)	0.56584
4th Feb 2021	Sentinel	NIR (Band 7)	Blue (Band 2)	0.83303
1st Mar 2021	Sentinel	NIR (Band 7)	Blue (Band 2)	0.84926
21st Mar 2021	Sentinel	SWIR (Band 11)	Blue (Band 2)	0.68939
24th Mar 2021	CubeSat	NIR (Band 4)	Blue (Band 2)	0.72240
26th Mar 2021	Sentinel	SWIR (Band 11)	Blue (Band 2)	0.75029
27th Mar 2021	CubeSat	NIR (Band 4)	Blue (Band 2)	0.73621

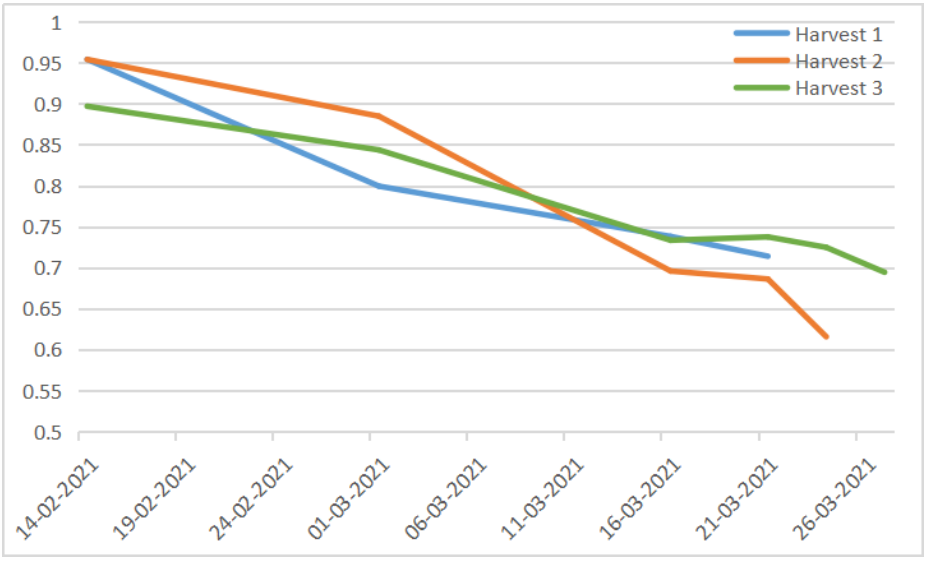

Figure 3. Temporal CBSI-MSAVI2 plots showing behaviour of crop fields from 14th Feb 2021 till the harvest dates i.e. 21st, 24th and 27th March 2021

Further MPCM algorithm was run for the three databases and results were obtained and the accuracy assessment was done on the basis of MMD and variance to check if the homogeneity within the mapped harvested fields and differentiation with respect to background.

5. Results and Discussion

Figures 4 and 5 show the fields harvested on 21st, 24th and 27th March 2021 overlaid on MSAVI2 image of the area using MSAVI2 index and CBSI-MSAVI2 index respectively for three different subsets of the study area.

(a)

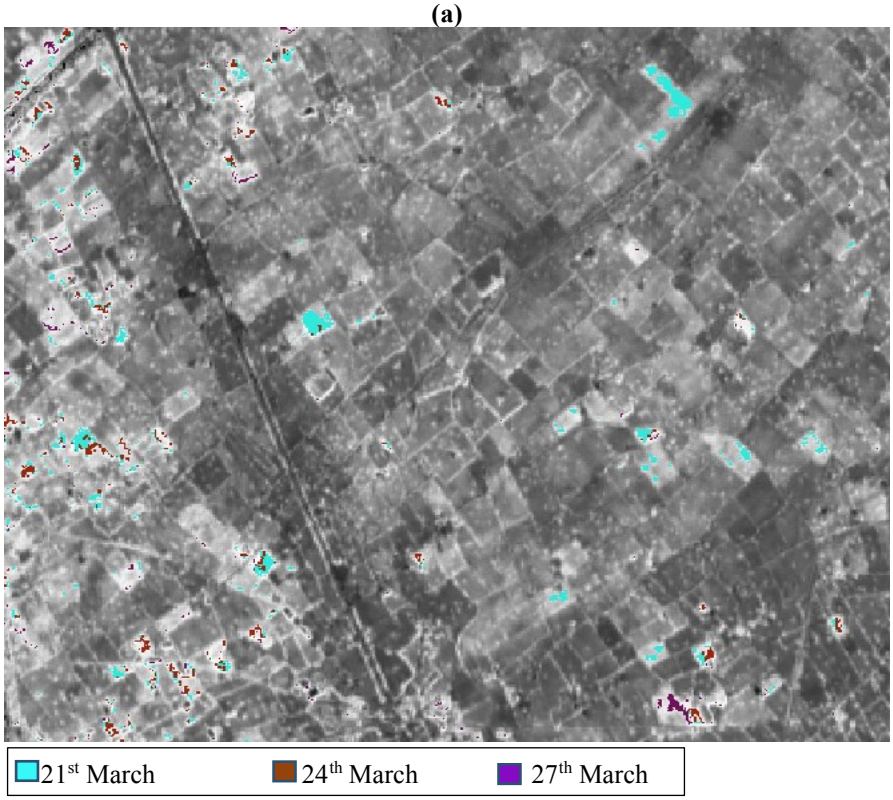

(b)

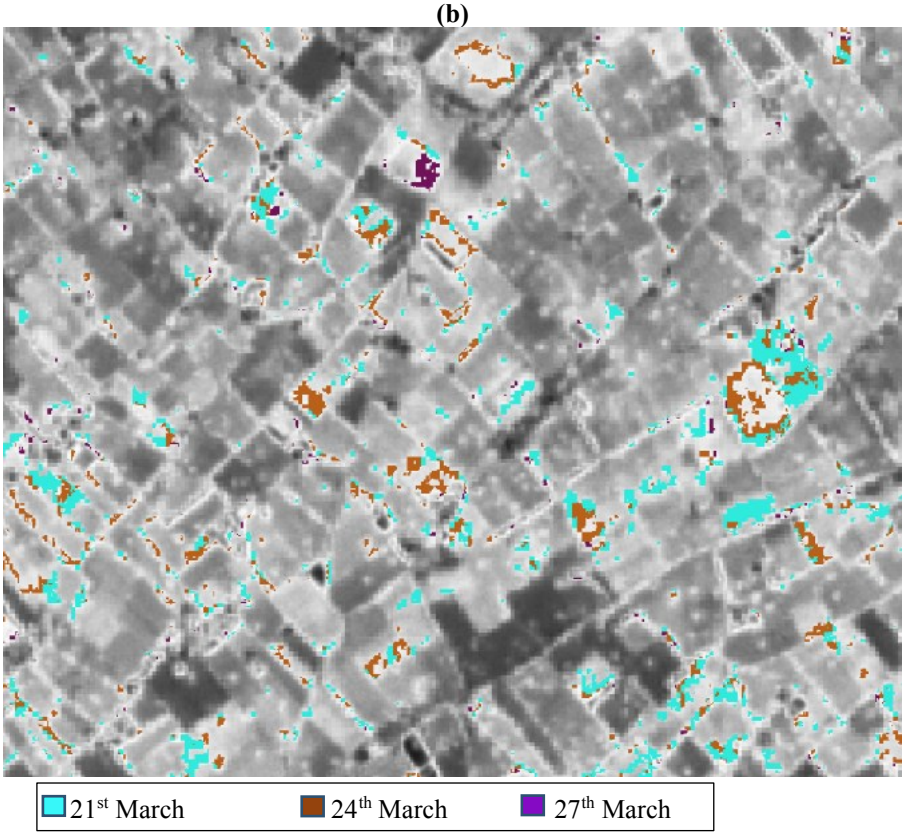

(c)

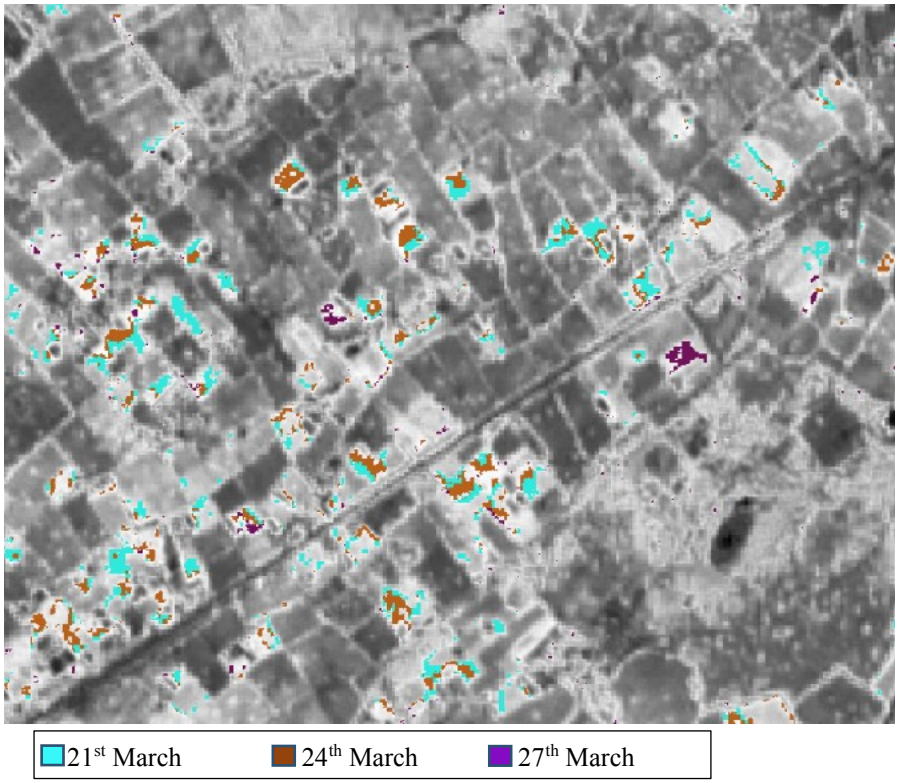

Figure 4. Fields harvested as mapped on 21st March, 24th March and 27th March using MSAVI2 using MPCM Mean Approach for three subsets of study area shown in (a), (b) and (c)

(a)

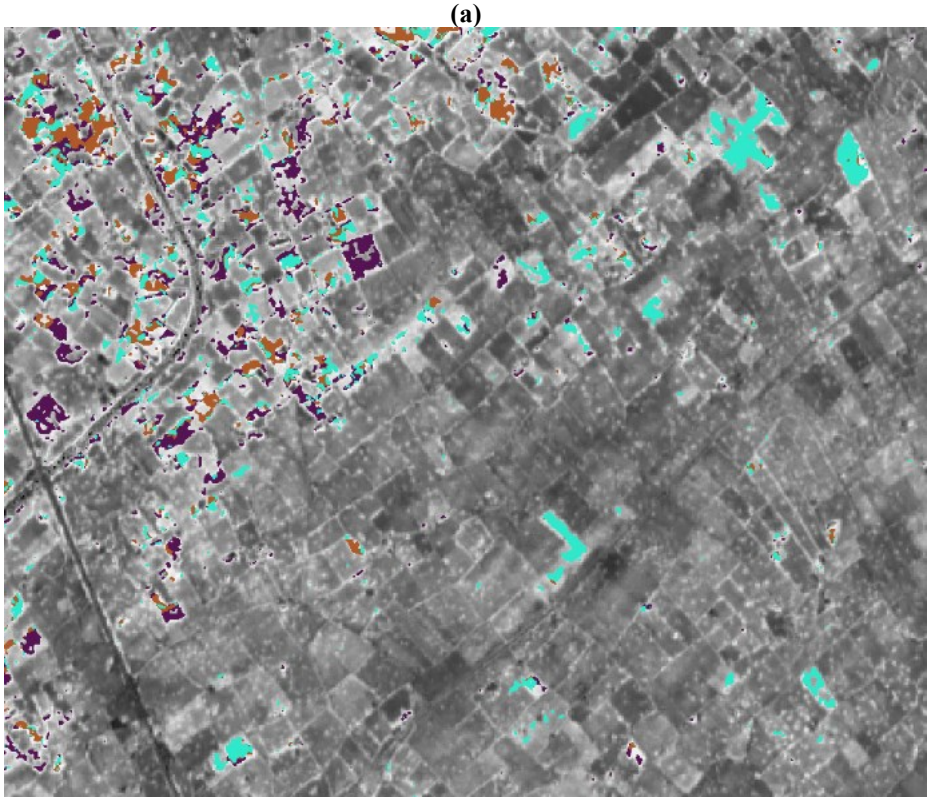
21st March
24th March
27th March

(b)

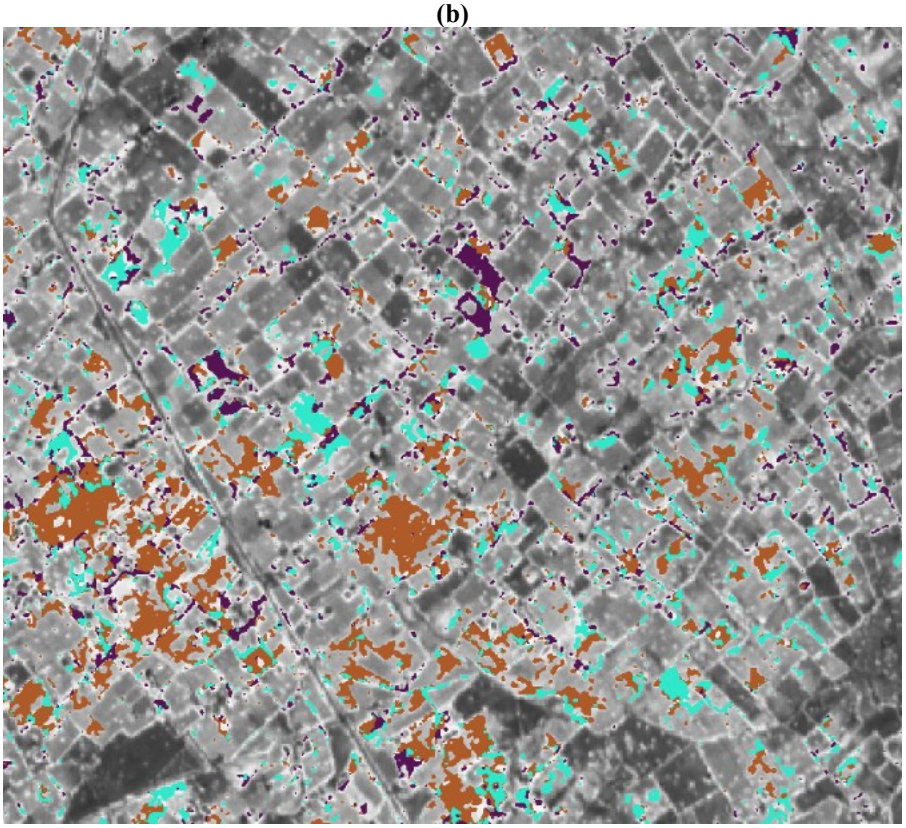
21st March
24th March
27th March

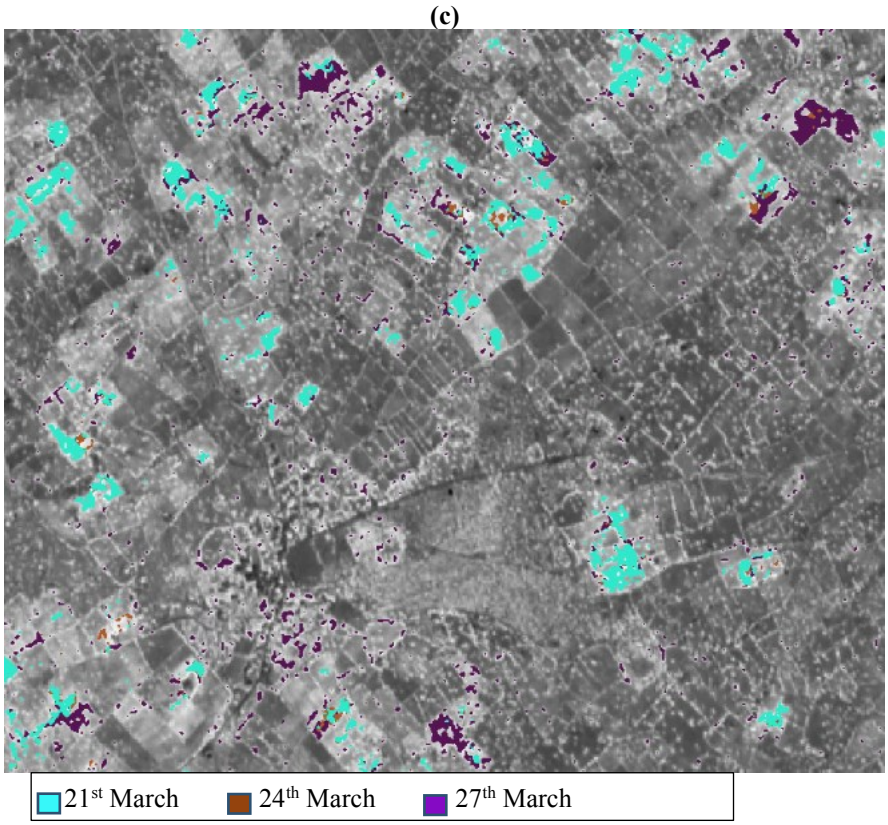

Figure 5. Fields harvested as mapped on 21st March, 24th March and 27th March using CBSI-MSAVI2 using MPCM Individual-sample-as-mean Approach for three subsets of study area shown in (a), (b) and (c)

It can be observed that the outputs for CBSI MSAVI2 are slightly better than that of conventional MSAVI2 in terms of delineation of harvested fields and the homogeneity within them. This may be due to the fact that CBSI approach works on the bands which specifically highlight the target crop by maximizing their MSAVI2 value while suppressing the background. The bands thus selected (as mentioned in Table 7) for dates under consideration support the application by effectively raising the MSAVI2 value for target class. Also it can be observed from Figure 3(b) that there is presence of some noise. This can be dealt with by application of smoothening filters such as median filter, which will remove this noise up to a large extent although on the cost of disturbance in the boundaries of correctly mapped fields.

Since the results for both the variants of index were in the form of fractional images, they were assessed on the basis of MMD (Mean Membership Difference) and variance within the target class. MMD basically shows the accuracy of algorithm in terms of its ability to differentiate between the target and non-target classes depending on the separation between membership values of the same. The MMD between target and non-target classes was supposed to be high since there must be a large gap between membership values of target (high) and non-target (low) classes. Whereas the MMD within the target crop itself should be as less as possible. This signifies that the pixels in the training and test field of the target crop have very close membership values. The variance within the target field should be minimum. It indicates the reduction in effect of heterogeneity within the target crop which may be a result of slight variations in the response of pixels in different parts of the target field due to change in availability of sunlight, water, pesticides, etc. Points distributed randomly throughout the field were considered and corresponding membership values were analyzed for the calculation of MMD and Variance. The results of MMD assessment (within crop and inter-crop) are shown in Table 8 along with the variance values of testing fields.

Table 8. Accuracy Assessment Results

Date	Approach	Mean Membership Values for Psyllium Husk crop		MMD Psyllium Husk crop	Variance Psyllium Husk crop
		Training Field	Testing Field		
21st March	MSAVI2	0.9725	0.9647	0.0078	0.00157
	CBSI MAVI2	0.9843	0.9804	0.0039	0.00031
24th March	MSAVI2	0.9882	0.9765	0.0117	0.001542
	CBSI MAVI2	0.9921	0.9843	0.0078	0.000542
27th March	MSAVI2	0.9336	0.9257	0.0021	0.02385
	CBSI MAVI2	0.9887	0.9605	0.0282	0.000141

As it can be observed from the results, both the techniques gave appreciable accuracy for different harvest dates in terms of MMD as well as variance. But the CBSI-MSAVI2 results show better homogeneity in output than that of MSAVI2 since the variance values were less comparatively.

Reliability of this technique can be checked with different crops. In the study area considered, other crops present can be tested such as Cumin, Fenugreek, taramira (Rocket leaves) (equivalent mustard crop) for monitoring of crops stages. It can also be used for judging impact of calamities or disease to estimate the loss occurred. This study can further be extended to different target features taking into consideration the appropriate band indices with CBSI approach to map the target.

References

Almutairi B., A. El, M. A. Belaid and N. Musa (2013). Comparative Study of SAVI and NDVI Vegetation Indices in Sulaibiya Area (Kuwait) Using Worldview Satellite Imagery. *International Journal of Geosceinces and Geomatics*, *1*(2), 50–53.

Bezdek J. C., R. Ehrlich and W. Full (1984). FCM: The fuzzy c-means clustering algorithm. *Computers & Geosciences*, *10*(2), 191–203. https://doi.org/https://doi.org/10.1016/0098-3004(84)90020-7

Biswas B., S. Walker and M. Varun (2017). Web GIS based identification and mapping of medicinal plants : A case study of Agra (U.P.), India. *Plant Archives*, *17*(1), 8–20.

Ennouri K., A. Kallel and R. Albano (2019). Remote sensing: An advanced technique for crop condition assessment. *Mathematical Problems in Engineering*, *2019*. https://doi.org/10.1155/2019/9404565

Huete A. R. (1996). A Soil-Adjusted Vegetation Index (SAVI). *Bangladesh Medical Research Council Bulletin*, *22*(1), 27–32.

Krishnapuram R. and J. M. Keller (1993). A possibilistic approach to clustering. *IEEE Transactions on Fuzzy Systems*, *1*(2), 98–110. https://doi.org/10.1109/91.227387

Krishnapuram Raghu and J. M. Keller (1996). The possibilistic C-means algorithm: Insights and recommendations. *IEEE Transactions on Fuzzy Systems*, *4*(3), 385–393. https://doi.org/10.1109/91.531779

Masood R. and M. Miraftab (2010). Psyllium: Current and Future Applications. *Medical and Healthcare Textiles*, 244–253. https://doi.org/10.1533/9780857090348.244

Murugan P., R. Sivakumar, R. Pandiyan and M. Annadurai (2016). Algorithm to select optimal spectral bands for hyperspectral index of feature extraction. *Indian Journal of Science and Technology*, *9*(37). https://doi.org/10.17485/ijst/2016/v9i37/85113

Qi J., A. Chehbouni, A. R. Huete, Y.H. Kerr and S. Sorooshian (1994). A modified soil adjusted vegetation index. *Remote Sensing of Environment*, *48*(2), 119–126. https://doi.org/10.1016/0034-4257(94)90134-1

Salmon J. M., M. A. Fried, S. Frolking, D. Wisser and E. M. Douglas (2015). Global rain-fed, irrigated, and paddy croplands: A new high resolution map derived from remote sensing, crop inventories and climate data. *International Journal of Applied Earth Observation and Geoinformation*, *38*, 321–334. https://doi.org/https://doi.org/10.1016/j.jag.2015.01.014

Sinha D. D. and Y. Singh (2011). *Mapping of Medicinal/Herbal Plant using Remote Sensing and GIS*.

Sun C., Y. Bian, T. Zhou and J. Pan (2019). Using of multi-source and multi-temporal remote sensing data improves crop-type mapping in the subtropical agriculture region. *Sensors (Switzerland)*, *19*(10), 1–23. https://doi.org/10.3390/s19102401

Verrelst J., J. P. Rivera, A. Gitelson, J. Delegido, J. Moreno and G. Camps-Valls (2016). Spectral band selection for vegetation properties retrieval using Gaussian processes regression. *International Journal of Applied Earth Observation and Geoinformation*, *52*, 554–567. https://doi.org/10.1016/j.jag.2016.07.016

Villa P., D. Stroppiana, G. Fontanelli, R. Azar and P.A. Brivio (2015). In-season mapping of crop type with optical and X-band SAR data: A classification tree approach using synoptic seasonal features. *Remote Sensing*, *7*(10), 12859–12886. https://doi.org/10.3390/rs71012859

Zhang T., J. Su, C. Liu, W. H.Chen, H. Liu and G. Liu (2017). Band selection in sentinel-2 satellite for agriculture applications. *2017 23rd International Conference on Automation and Computing (ICAC)*, 1–6. https://doi.org/10.23919/IConAC.2017.8081990

Zhou T., Z. Li and J. Pan (2018). Multi-feature classification of multi-sensor satellite imagery based on dual-polarimetric sentinel-1A, landsat-8 OLI, and hyperion images for urban land-cover classification. *Sensors (Switzerland)*, *18*(2), 1–20. https://doi.org/10.3390/s18020373